

Modulated Predictive Controller for a Single-Phase Cascaded Transformer Multilevel Inverter

Gleice Mylena da S. Rodrigues*, Nady Rocha*, Ilaneide Jaqueline do N. Silva*,
Edison Roberto C. da Silva* and Victor Felipe M. B. Melo*

*Dept. of Electrical Engineering

Federal University of Paraiba, Joao Pessoa, Paraiba

Email: [gleice.rodrigues, nadyrocha, ilaneide.silva, edison.roberto, victor]@cear.ufpb.br

Abstract—In this paper, the modulated model predictive control (M²PC) of a cascaded transformer multilevel inverter (CTMI) is considered and designed to regulate the load current. The future value of the load current is obtained from a discrete-time model of the system. A five-level load voltage can be achieved. The M²PC preserves the advantages of conventional model predictive control and, due to the modulator based on space vector modulation, this technique uses a fixed switching frequency, minimizing the harmonic distortion of voltage and current and decreasing the switching losses. However, the voltages waveform at primary side may have a DC-component that leads to core saturation of the transformer. In order to eliminate the DC components and reduce the complexity of the controller, the cost function is calculated for a set of preselected vectors of the system. Finally, the performance of the predictive control is verified by both simulation and experimental results.

Keywords – cascaded transformer multilevel inverter, model predictive control, modulated model predictive control.

I. INTRODUCTION

The most popular multilevel inverter topologies are diode clamped (NPC), flying capacitors (FCs) and cascaded H-bridge (CHB) converter with separate DC-sources. Multilevel topologies have a number of advantages, such as low dv/dt stress on switches, reduced electromagnetic interference (EMI), lower switching losses, lower harmonic distortion, and higher power quality [1]–[3]. The cascaded H-bridge (CHB) multilevel inverter is well known, being widely used in industrial applications, such as synchronous motors and power generation plants. This happens because the CHB converter has as advantages a simple control strategy and requires a lower number of semiconductor devices to generate a particular number of levels when compared to the other structures. However, the CHB converter needs several isolated DC-link sources [1]–[3].

This problem can be solved by employing Cascaded Transformer Multilevel Inverter (CTMI). It consists of H-bridge converters connected to the primary winding of low-frequency transformers, while the secondary windings are connected in series. Different from CHB inverter, the CTMI needs only one DC-link source [2]. Also, In applications such as photovoltaic panels and dynamic voltage restorer (DVR) an isolation transformer is required. Then, besides ensuring a galvanic isolation between load and converter, the transformers can

minimize leakage current in photovoltaic systems. In addition, the leakage inductances of the transformers can be used as a current filter without the need for an extra filter or can minimize the size of the filter.

An important topic in power electronics is the converter control technique. Different control techniques have been proposed and studied in the technical literature. Among the several control methods applied in power electronics, the following stand out: fuzzy control, sliding mode control and predictive control. The Model Predictive Control (MPC) is one of the most popular control system applied in engineering. The MPC is a feedback control that uses the system model to predict the future behavior of the variables under control [4]–[7]. Some MPC advantages are good dynamic response and possibility of incorporating multiple control objectives. A disadvantage of predictive control is a high computational cost. However, the development of powerful microprocessors and field-programmable gate arrays (FPGAs) have made possible the application of MPC in power electronics [8], [9].

Recent studies have led to a variation of the MPC method, called Modulated Model Predictive Control (M²PC), with the inclusion of a modulation system. This variation aims to improve the system performance in terms of power quality while maintaining the advantages of traditional MPC [10], [11]. This technique has been applied for the control of three-phase converter [11], shunt active power filter [12], permanent magnet machine [10] and Multilevel AC/AC Converter [13]. In [11] the M²PC is applied to the current control of a three-phase rectifier. In this paper the Space vector modulation (SVM) has been adopted as modulator, which guarantees a fixed switching frequency, as also reduced harmonic distortion and switching losses when compared to traditional MPC.

In this paper, the current control of a cascaded transformer multilevel inverter using the modulated model predictive control (M²PC) is considered. The CTMI uses two H-bridge inverters with two cascaded transformers and only one single DC-link voltage source. The primary windings of the transformers are connected to inverters, while the secondary windings are connected to the load. Cascaded transformer multilevel inverter generates a load voltage with five-level when identical transformer ratios are used. The M²PC preserves the advantages of conventional model predictive control method and, due to modulator based on space vector modulation, this

technique uses a fixed switching frequency, minimizes the harmonic distortion of the voltage and current and, decreases the switching losses. Regardless of the voltages waveform at primary side, they can present a DC-component that leads to transformer core saturation. Aiming to eliminate DC components and reduce controller complexity, preselected system vectors are used in the cost function calculation. Simulation and experimental results validate the predictive current control performance applied to the cascaded transformer multilevel inverter.

II. SYSTEM MODEL

The CTMI analyzed here consists of a single DC-link voltage, two low frequency transformers, and two full-bridge converters, as shown in Fig. 1(a). From Fig. 1(a), the basic module of the full-bridge converter is connected to a low-frequency transformer. Assuming that the transformer ratio is $n_a:n_b$, where n_a (N_{a2}/N_{a1}) is the transformer ratio of the transformer T_a and n_b (N_{b2}/N_{b1}) is the transformer ratio of the transformer T_b . In the relation 1:1, the transformers have an identical transformer ratio, being called as symmetric topology.

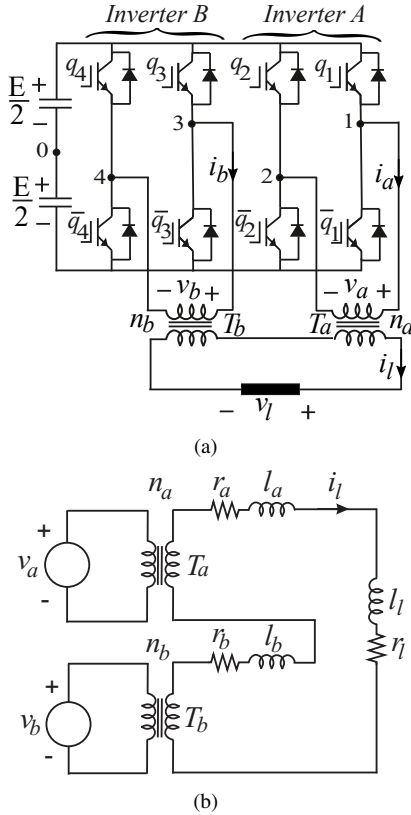


Fig. 1. (a) CTMI configuration. (b) CTMI equivalent circuit.

The model of converter shown in Fig. 1(a) is given by:

$$v_a = v_{10} - v_{20} \quad (1)$$

$$v_b = v_{30} - v_{40} \quad (2)$$

where v_a and v_b are the converter voltages, v_{10} to v_{40} are the pole voltages.

At the load side, the equivalent model is shown in Fig. 1(b). A simplified transformer model was used, in which the magnetizing branch was neglected, due to its low impact on the system model, and the primary inductance of the transformer can be transferred to the secondary side, so that, the two inductances can be represented as an equivalent leakage inductance at the secondary side. From Fig. 1(b) the following equations can be derived

$$n_a v_a + n_b v_b = (r_a + r_b + r_l) i_l + (l_a + l_b + l_l) \frac{di_l}{dt} \quad (3)$$

where r_a and r_b represent the equivalent resistance of the transformers T_a and T_b , respectively, l_a and l_b represent the equivalent leakage inductance of the transformers T_a and T_b , respectively, r_l and l_l represent the resistance and inductance of the load and i_l is the load current.

In this way the load current dynamics can be described by an equivalent equation

$$v_l = R i_l + L \frac{di_l}{dt} \quad (4)$$

where $v_l = n_a v_a + n_b v_b$, $R = r_a + r_b + r_l$ and $L = l_a + l_b + l_l$.

From (1) and (2), it is possible to write the converter voltages as a function of the switching states and the DC-link voltage, that is

$$v_a = (q_1 - q_2) E \quad (5)$$

$$v_b = (q_3 - q_4) E \quad (6)$$

where q_1 to q_4 are the state of the switches of the cascaded transformer multilevel inverter and E is the DC-link voltage. There are sixteen possible switching states for CTMI and using the transformer ratio 1:1 is possible to achieve multilevel load voltage with five-level, as shown in Table I.

TABLE I
SWITCHING STATES AND OUTPUT LOAD VOLTAGE FOR TRANSFORMER RATIO 1:1.

Switching State				Transformer voltages		Output load voltages
q_1	q_2	q_3	q_4	v_a	v_b	$v_l (n_a : n_b = 1 : 1)$
0	0	0	0	0	0	0
0	0	0	1	0	-E	-E
0	0	1	0	0	E	E
0	0	1	1	0	0	0
0	1	0	0	-E	0	-E
0	1	0	1	-E	-E	-2E
0	1	1	0	-E	E	0
0	1	1	1	-E	0	-E
1	0	0	0	E	0	E
1	0	0	1	E	-E	0
1	0	1	0	E	E	2E
1	0	1	1	E	0	E
1	1	0	0	0	0	0
1	1	0	1	0	-E	-E
1	1	1	0	0	E	E
1	1	1	1	0	0	0

III. DISCRETE MODEL

A discrete-time form of the load current (4) for a sampling time T_s can be used to predict the future value of load current from the measured load current (i_l). The derivative current can be approximated by the implicit Euler scheme, i.e.,

$$\frac{di_l}{dt} \approx \frac{i_l(k) - i_l(k-1)}{T_s} \quad (7)$$

From (7) and (4) the following expression can be obtained for the discretized load current:

$$i_l(k) = \frac{1}{L + RT_s} [T_s v_l(k) + Li_l(k-1)] \quad (8)$$

The load current in the future, which is the predicted current, is obtained by changing the discrete time to one step forward.

$$i_l(k+1) = \frac{1}{L + RT_s} [T_s v_l(k+1) + Li_l(k)] \quad (9)$$

In order to prevent a computational delay presents in the experimental set-up, the predictive current is evaluated at the instant $k+2$, i.e., two steps ahead [10], [11]. In this way, assuming that $v_l(k+2) = v_l(k+1)$ for a small sampling time T_s , the current at the instant $k+2$ can be predicted as

$$i_l(k+2) = \frac{1}{L + RT_s} [T_s v_l(k+1) + Li_l(k+1)] \quad (10)$$

IV. MODULATED PREDICTIVE CONTROL STRATEGY

Fig. 2 shows the predictive control block diagram of the cascaded transformer multilevel inverter. The predictive current in the next sampling interval $i_l(k+2)$ is defined by the discrete-time model of the CTMI from Fig. 2, being represented by block Predictive Model. The space vector modulation (SVM) for single-phase converter is based on one dimensional (1D) control region [14]. It is possible to define each available vector for the CTMI in a line as shown in Fig. 3. Ideally, the CTMI is capable of generating an output voltage with five levels: $-2E$, $-E$, 0 , E and $2E$. From Fig. 3, it is possible to define four different sectors (Sectors I, II, III and IV) which are given by two adjacent vectors. In the level voltages $-E$, 0 and E , the presence of redundant state vectors is clear.

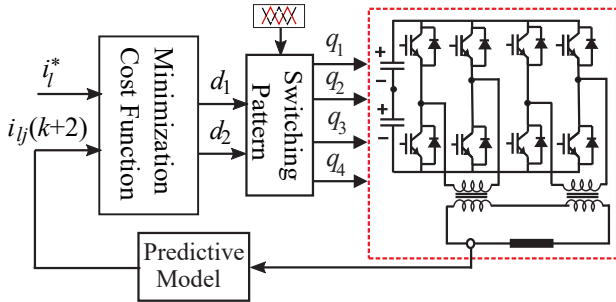


Fig. 2. Control block diagram.

The SVM was developed using two adjacent vectors in each sector, being possible to obtain a total of 56 switching combinations. As an example, for sector I, using two adjacent

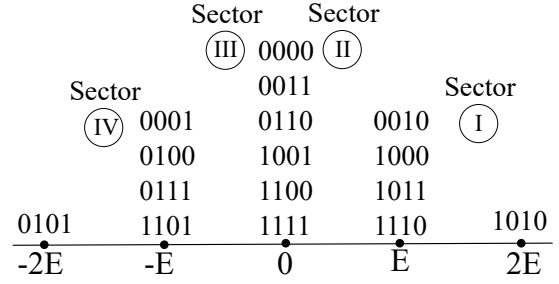


Fig. 3. One-dimensional control region.

vectors, four different state vectors are available, i.e., 1010-0010, 1010-1000, 1010-1011, 1010-1110. To avoid increasing the complexity of the controller, the cost function is calculated for a set of preselected vectors. In this way, the adjacent vectors are selected in order to produce the minimum number of switching events. Table II shows the switching transitions for each sector of all possible combinations of switching states when only one switch changes its state. When this switch changes its state from high to low ($1 \Rightarrow 0$), this pair of adjacent vectors is classified as high-to-low, while if its state changes from low to high ($0 \Rightarrow 1$) this pair of adjacent vectors is classified to low-to-high, as illustrated in Table II. As an example, the adjacent vectors 1010-0010 is classified as high-to-low, because the state of q_1 changes from high to low ($q_1 = 1 \Rightarrow q_1 = 0$), while the other switches do not change their states.

TABLE II
ADJACENT VECTORS WITH MINIMUM NUMBER OF SWITCHING EVENTS.

Sector	Vector High-to-Low	Vector Low-to-High
I	1010 \Rightarrow 0010	1010 \Rightarrow 1011
	1010 \Rightarrow 1000	1010 \Rightarrow 1110
II	0010 \Rightarrow 0000	0010 \Rightarrow 0011
	1000 \Rightarrow 0000	0010 \Rightarrow 0110
	1011 \Rightarrow 0011	1000 \Rightarrow 1001
	1011 \Rightarrow 1001	1000 \Rightarrow 1100
	1110 \Rightarrow 0110	1011 \Rightarrow 1111
III	1110 \Rightarrow 1100	1110 \Rightarrow 1111
	0011 \Rightarrow 0001	0000 \Rightarrow 0001
	1001 \Rightarrow 0001	0000 \Rightarrow 0100
	0110 \Rightarrow 0100	0011 \Rightarrow 0111
	1100 \Rightarrow 0100	0110 \Rightarrow 0111
IV	1111 \Rightarrow 0111	1001 \Rightarrow 1101
	1111 \Rightarrow 1101	1100 \Rightarrow 1101
	0111 \Rightarrow 0101	0001 \Rightarrow 0101
	1101 \Rightarrow 0101	0100 \Rightarrow 0101

The Modulated Predictive Control Strategy (M^2PC) is similar to classic Model Predictive Control, i.e., from discrete model, the predictive current and cost function are calculated [15]. Moreover, the M^2PC calculates the predicted current and the cost function for all two adjacent vectors of each sector and the pair of vectors that minimizes the cost function is selected. For example, from Table II and sector I, when high-to-low vector is used, one possibility is first calculating cost function g_1 using vector 1010 and then calculating cost function g_2 for vector 0010.

The cost function (g_j , with $k=1,2$) used for this application is based on the absolute error:

$$g_j = |i_l^* - i_l(k+2)| \quad (11)$$

where i_l^* is the reference load current.

The M²PC is based on calculus of the duty cycle related to the two adjacent vectors. As shown in [15], [16], the duty cycles (d_1 and d_2) can be calculated by:

$$d_1 = \frac{g_2}{g_1 + g_2} \quad (12)$$

$$d_2 = \frac{g_1}{g_1 + g_2} \quad (13)$$

The cost function is evaluated for sixteen pairs of adjacent vectors. The pair of vectors that minimizes it is chosen and applied in the next control period. The cost function is calculated by:

$$g = d_1 g_1 + d_2 g_2 \quad (14)$$

In order to reduce the complexity of the controller, only sixteen different pairs of adjacent state vectors are applied. However, when only vectors high-to-low or low-to-high are used, unfortunately, a DC-component comes up in the currents at the primary side of the transformers. The DC-component in the transformers winding leads to the transformer core saturation. This is a serious problem that can happen in the transformer [3]. In order to eliminate the DC-component, vectors low-to-high are used in sectors I and II, while vectors high-to-low are used in sectors III and IV, or vice-versa.

Fig. 4 illustrates the flowchart of the control system. Initially, the load current at the secondary side of the transformer is measured. In the *for* loop, the predictive algorithm chooses, among the sixteen pairs of adjacent state vectors, the voltages $v_{aj}(k+1)$ and $v_{bj}(k+1)$ to be applied to each transformer, as calculated in (5) and (6). After that, the predictive currents $i_{lj}(k+2)$ are calculated from the discrete-model in (10) for the chosen pair of adjacent vectors. From the predictive currents, the cost functions g_1 and g_2 are calculated from (11), and the duty cycles d_1 and d_2 are evaluated by (12) and (13). Then, the duty cycles d_1 and d_2 that minimize the cost function g are selected. After obtaining the duty cycles, the gating signals are obtained comparing the duty-cycle with a double high frequency triangular carrier signal, i.e., double-carrier-based PWM. In the case of double-carrier based PWM, the phase shift of the triangular carrier signals between high-to-low and low-to-high vectors is 180° .

V. SIMULATION RESULTS

In order to demonstrate the feasibility of the cascaded multilevel converter using predictive control, digital simulations have been performed. The results were obtained for the following conditions: the DC-link voltage is equal to 100 V, reference current amplitude is equal to 1 A, the capacitance of DC-link is equal to 4400 μF ; the sampling time is equal to 100 μs and the transformers parameters are given in Table III. A RL load was used with $R = 150 \Omega$ and $L = 20 mH$.

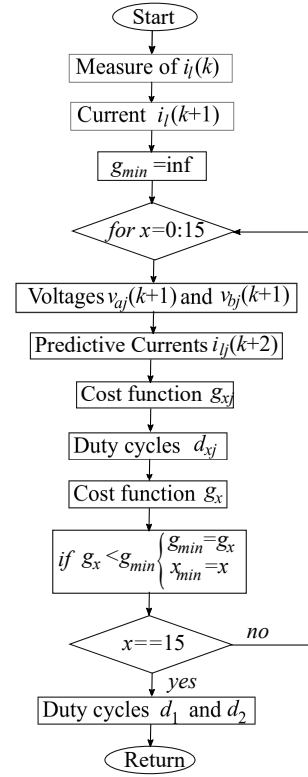


Fig. 4. The flowchart of the CTMI.

Vectors low-to-high have been used in sectors I and II; instead vectors high-to-low have been used in sectors III and IV.

TABLE III
TRANSFORMER PARAMETERS.

Transformer 1:1	
Parameters	Values
r_p (primary)	0.2687 Ω
r_s (secondary)	0.2687 Ω
l_p (pri. leakage)	0.0714 mH
l_s (sec. leakage)	0.0714 mH
l_m (magnetizing)	5.7443 H

Fig. 5 illustrates the performance of the cascaded transformer multilevel inverter under predictive control. Fig. 5(a) (bottom) shows that the load voltage has five levels, with a Weighted Total Harmonic Distortion (WTHD) equals to 0.20 %. Fig. 5(a) (top) shows that the load current is sinusoidal with 60 Hz fundamental frequency and Total Harmonic Distortion (THD) equals to 3.81 %. The currents at the primary side of the transformers are shown in Fig. 5(c). It is worth noting that there is no DC-component at the currents. This happens because the shapes of the transformer voltages v_a and v_b generated by optimized states vectors suppress the DC-component, as illustrated in Fig. 5(b). The shape of voltage at positive and negative sides is similar. It can be noted that the converter A has a low switching frequency, while the converter B has a high switching frequency. This is due to the evaluation performed by the cost function of pre-selected

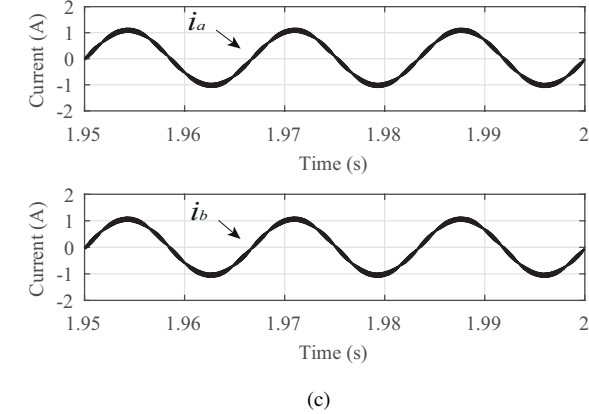
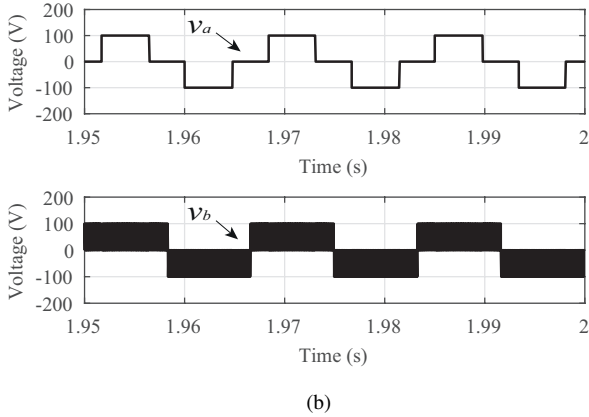
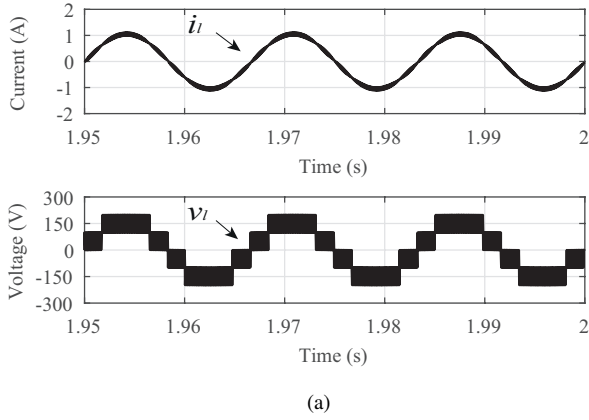


Fig. 5. Simulation results: (a) Load current (top) and load voltage (bottom). (b) Transformer voltages (v_a and v_b). (c) Transformer currents at the primary side (i_a and i_b).

adjacent vectors in order to minimize the required processing time of the algorithm and the number of switching events.

VI. EXPERIMENTAL RESULTS

The proposed system has been implemented in the laboratory using the power converters shown in Fig. 6. The experimental set-up is based on a Digital Signal Processor (DSP) TMS320F28335 with a microcomputer equipped with appropriate plug-in boards and sensors. The results were

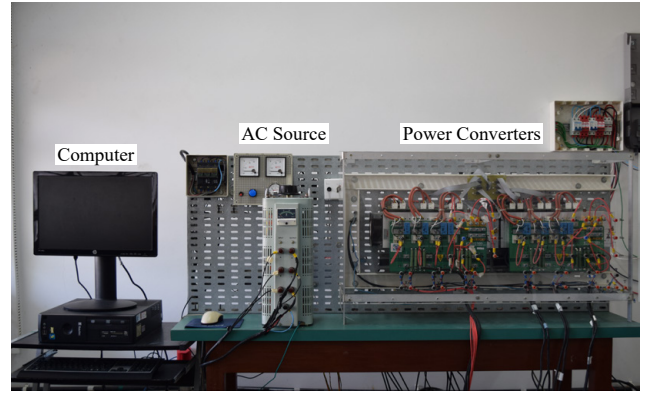


Fig. 6. Experimental setup.

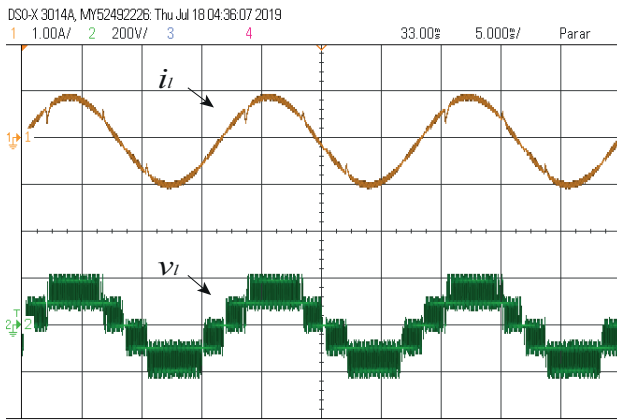
obtained by oscilloscope Agilent DSO-X 3014A 100 MHz. The switching frequency is equal to 10 kHz, the DC-link voltage is equal to 100 V and the DC-link capacitance is equal to 4400 μ F. A three-phase RL load of 150 Ω and 20 mH was used.

The steady-state waveforms for load current, load voltage, transformer voltages and converter currents using the modulated model predictive control are shown in Fig. 7. In these results the amplitude of reference load current was equal to 1 A. Notice that the control guarantees sinusoidal current and load voltage with five-level step [see Fig. 7(a)]. The pair of adjacent vectors applied guarantees the converter A to operate with three-step voltage and low switching frequency while the converter B works with high switching frequency, as shown in Fig. 7(b). Fig. 7(c) shows the transformer currents at the primary side. It is worth noting that there is no DC-component at the currents. This happens because the shapes of the transformer voltages v_a and v_b are generated by optimized states vectors that suppress the DC-component.

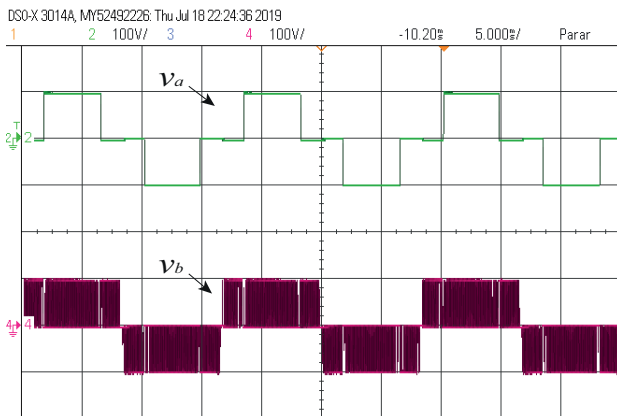
VII. CONCLUSION

This paper presented a modulated model predictive control for a single-phase cascaded transformer multilevel inverter. The M²PC has already been introduced in previous works, highlighting the advantages of this technique over conventional full proportional-integral (PI) control scheme, in relation to the fast dynamic response [10] and constant switching frequency in comparison with the traditional MPC [11].

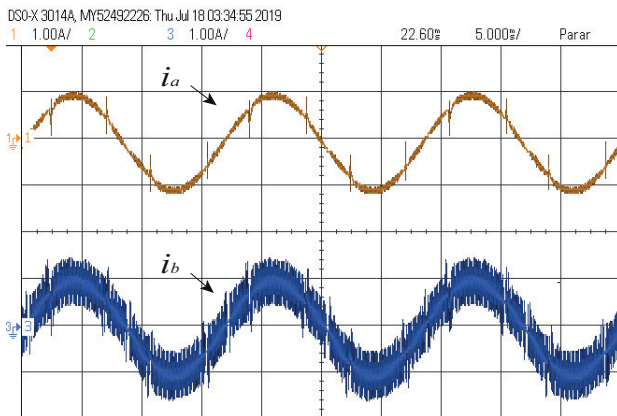
The CTMI analysed here uses two H-bridge converters with two cascaded transformers and only one single DC-link voltage source. The primary windings of the transformers are connected to H-bridge inverters, while the secondary windings are connected to the load. A five-level load voltage was achieved, using transformer ratios equal to 1:1. In order to reduce the complexity of the controller and eliminate the DC-component, only sixteen different pairs of adjacent state vectors have been applied. Vectors high-to-low are used in sectors I and II, while vectors low-to-high are used in sectors III and IV, or vice-versa. The pair of adjacent vectors guaranteed a three-step voltage with low switching frequency for converter



(a)



(b)



(c)

Fig. 7. Experimental results. (a) Current and voltage of the load (i_l and v_l). (b) Transformer voltages (v_a and v_b). (c) Transformer currents at the primary side (i_a and i_b).

A, while the converter B works with high switching frequency. Simulation and experimental results were presented for the proposed validation.

ACKNOWLEDGMENT

The authors would like to thank in part the Coordenação de Aperfeiçoamento de Pessoal de Nível Superior - Brasil

(CAPES) and the Conselho Nacional de Desenvolvimento Científico e Tecnológico CNPq for the financial support.

REFERENCES

- [1] A. Ajami, A. Farakhor, and H. Ardi, "Minimisations of total harmonic distortion in cascaded transformers multilevel inverter by modifying turn ratios of the transformers and input voltage regulation," *IET Power Electronics*, vol. 7, no. 11, pp. 2687–2694, 2014.
- [2] H. Khoum jahan, K. Zare, and M. Abapour, "Verification of a low component nine-level cascaded-transformer multilevel inverter in grid-tied mode," *IEEE Journal of Emerging and Selected Topics in Power Electronics*, vol. 6, no. 1, pp. 429–440, March 2018.
- [3] H. K. Jahan, M. Naseri, M. M. Haji-Esmaili, M. Abapour, and K. Zare, "Low component merged cells cascaded-transformer multilevel inverter featuring an enhanced reliability," *IET Power Electronics*, vol. 10, no. 8, pp. 855–862, 2017.
- [4] S. Vazquez, C. Montero, C. Bordons, and L. G. Franquelo, "Model predictive control of a vsi with long prediction horizon," in *2011 IEEE International Symposium on Industrial Electronics*, June 2011, pp. 1805–1810.
- [5] S. Kouro, P. Cortes, R. Vargas, U. Ammann, and J. Rodriguez, "Model predictive control—a simple and powerful method to control power converters," *IEEE Transactions on Industrial Electronics*, vol. 56, no. 6, pp. 1826–1838, June 2009.
- [6] P. Cortes, L. Vattuone, and J. Rodriguez, "A comparative study of predictive current control for three-phase voltage source inverters based on switching frequency and current error," in *Proceedings of the 2011 14th European Conference on Power Electronics and Applications*, Aug 2011, pp. 1–8.
- [7] Y. Zhang, R. Kotecha, H. A. Mantooth, J. C. Balda, Y. Zhao, and C. Farnell, "Cascaded bridgeless totem-pole multilevel converter with model predictive control for 400 v dc-powered data centers," in *2017 IEEE Applied Power Electronics Conference and Exposition (APEC)*, March 2017, pp. 2745–2750.
- [8] S. Vazquez, J. I. Leon, L. G. Franquelo, J. Rodriguez, H. A. Young, A. Marquez, and P. Zanchetta, "Model predictive control: A review of its applications in power electronics," *IEEE Industrial Electronics Magazine*, vol. 8, no. 1, pp. 16–31, March 2014.
- [9] R. O. Ramirez, J. R. Espinoza, P. E. Melin, M. E. Reyes, E. E. Espinosa, C. Silva, and E. Maurelia, "Predictive controller for a three-phase/single-phase voltage source converter cell," *IEEE Transactions on Industrial Informatics*, vol. 10, no. 3, pp. 1878–1889, Aug 2014.
- [10] S. S. Yeoh, T. Yang, L. Tarisciotti, C. I. Hill, S. Bozhko, and P. Zanchetta, "Permanent-magnet machine-based starter-generator system with modulated model predictive control," *IEEE Transactions on Transportation Electrification*, vol. 3, no. 4, pp. 878–890, Dec 2017.
- [11] L. Tarisciotti, P. Zanchetta, A. Watson, J. C. Clare, M. Degano, and S. Bifaretti, "Modulated model predictive control for a three-phase active rectifier," *IEEE Transactions on Industry Applications*, vol. 51, no. 2, pp. 1610–1620, March 2015.
- [12] L. Tarisciotti, A. Formentini, A. Gaeta, M. Degano, P. Zanchetta, R. Rabbeni, and M. Pucci, "Model predictive control for shunt active filters with fixed switching frequency," *IEEE Transactions on Industry Applications*, vol. 53, no. 1, pp. 296–304, Jan 2017.
- [13] Z. He, P. Guo, Z. Shuai, Q. Xu, A. Luo, and J. M. Guerrero, "Modulated model predictive control for modular multilevel ac/ac converter," *IEEE Transactions on Power Electronics*, vol. 34, no. 10, pp. 10359–10372, Oct 2019.
- [14] J. I. Leon, S. Vazquez, A. J. Watson, L. G. Franquelo, P. W. Wheeler, and J. M. Carrasco, "Feed-forward space vector modulation for single-phase multilevel cascaded converters with any dc voltage ratio," *IEEE Transactions on Industrial Electronics*, vol. 56, no. 2, pp. 315–325, Feb 2009.
- [15] M. Rivera, M. Perez, V. Yaramasu, B. Wu, L. Tarisciotti, P. Zanchetta, and P. Wheeler, "Modulated model predictive control (m2pc) with fixed switching frequency for an npc converter," in *2015 IEEE 5th International Conference on Power Engineering, Energy and Electrical Drives (POWERENG)*, May 2015, pp. 623–628.
- [16] L. Tarisciotti, P. Zanchetta, A. Watson, P. Wheeler, J. C. Clare, and S. Bifaretti, "Multiobjective modulated model predictive control for a multilevel solid-state transformer," *IEEE Transactions on Industry Applications*, vol. 51, no. 5, pp. 4051–4060, Sep. 2015.